Communication

Study of the Conformation of Bromated Guanidines with Potential Anti-leishmania Activity

Eduardo Henrique Zampieri , Luana Ribeiro Dos Anjos , Pedro Henrique de Oliveira Santiago , Tainara Rosário da Silva Nascimento , Javier Ellena , Eduardo René Pérez González *

Posted Date: 26 February 2024

doi: 10.20944/preprints202312.1728.v2

Keywords: Guanidines compounds; Leishmaniasis; Bromination; NBS; X-ray and NMR conformational study.

Article

Study of the Conformation of Bromated Guanidines with Potential Anti-leishmania Activity

Eduardo Henrique Zampieri [1], Luana Ribeiro dos Anjos [1], Pedro Henrique de Oliveira Santiago [2], Tainara Rosário da Silva Nascimento [1], Javier Alcides Ellena [2] and Eduardo René Pérez González [1, *]

[1] Fine Organic Chemistry Lab, School of Sciences and Technology, São Paulo State University (UNESP), Presidente Prudente 19060-080, Brazil; eduardo.h.zampieri@unesp.br, luana.anjos@unesp.br, tainara.nascimento@unesp.br
[2] Multiuser Structural Crystallography Laboratory, São Carlos Institute of Physics, University of São Paulo (USP), São Carlos 13566-590, Brazil; pedrophs.santiago@gmail.com, javiere@if.sc.usp.br
* Correspondence: eduardo.gonzalez@unesp.br

Abstract: Leishmaniasis are neglected diseases that affect regions such as South Asia, South Africa and Latin America, less developed regions. Current treatment, for cutaneous, mucocutaneous and visceral leishmaniosis, which are the main forms of the disease, is based on the administration of pentavalent antimonial and amphotericin B. However, these drugs have low efficacy and high toxicity. For this reason, the search for new treatments for this disease is necessary, based on studies of new molecules and their conformations. The research proposed the conformational study of brominated guanidine compounds with potential antileishmanial activity using Nuclear Magnetic Resonance (NMR) and X-ray diffraction (XRD) techniques. The present study involves the brominated molecules, LQOF-G2, LQOF-G30, LQOF-G35 and LQOF-G35-Br. The later was synthesized by the reaction of LQOF-G35 with NBS under IR irradiation at 120 Watts of potency and dichloromethane as solvent by 12-h of exposition. The obtained results demonstrated the efficiency of the bromination method, since two bromines atoms entered the molecule. Furthermore, NMR analysis showed the occurrence of a conformational change from Z to E when compound LQOF-G35 was brominated to LQOF-G35-Br. This feature was well confirmed by comparative DRX study of the LQOF-G35 and LQOF-G35-Br compounds. The antileishmanial activity of LQOF-G2 e LQOF-G35 motivated the synthesis of new brominated compounds LQOF-G30 e LQOF-G35-Br.

Keywords: Guanidines compounds; Leishmaniasis; Bromination; NBS; X-ray and NMR conformational study

1. Introduction

The research and development of drugs to treat diseases, such as leishmaniasis, involves the creation of molecules through pharmacological design, synthesis, and biological and structural characterization. Leishmaniasis, prevalent in Southeast Asia, Sub-Saharan Africa and Latin America [1], encompasses several clinical-pathological manifestations, among them the most common known as cutaneous leishmaniasis, caused by *Leishmania amazonensis*, manifests itself through lesions and ulcers on the skin, and the most severe, visceral leishmaniasis, is characterized by anemia, significant weight loss, enlarged spleen, fever and often results in death, the latter being observed in 85-90% of untreated cases [1,2,3].

Current treatments, such as chemotherapy with pentavalent antimonial compounds, paromomycin, amphotericin B, and miltefosine, present challenges, including low efficacy and severe side effects such as cardiotoxicity, pancreatitis, hepatotoxicity, parasite resistance, and long-term administration [2-5]. Therefore, the search for safer and more effective antileishmanial compounds is essential [4,5,6].

Guanidine compounds are often found in nature and used in the synthesis of a variety of organic compounds, such as quinazolines, oxazolidinones, lactones, and carbonates [7-11]. Novel guanidine derivatives exhibit several biological effects, such as cardiovascular dilation, antihistamine properties, anti-inflammatory activity, antidiabetic effects, antibacterial, antifungal,

 doi:10.20944/preprints202312.1728.v2

antiprotozoal/antiparasitic properties, and antiviral activity [7,12-21]. Recently, some guanidine compounds have been studied in relation to leishmaniasis [22,23].

In 2019, Espírito Santo R. D. *et al.*, carried out the structural characterization by nuclear magnetic resonance (NMR) and the evaluation of the antiparasitic activity of a series of guanidine compounds [20], in this study some compounds proved to be highly effective and promising due to their low toxicity against mammals and high lethality for parasites. The most important compound was LQOF-G2, which has a bromine atom in the "*para*" position of the aniline ring.

LQOF-G2 shows a preferential '*Z*' conformation being observed and *in vivo* activity [20]. Recently a new guanidine compound, LQOF-G35, which has a bromine atom as a substituent in the "*ortho*" position of the aniline ring, has showed activity against *Leishmania braziliensis* [24].

These benzoylguanidines had their *E*/*Z* isomerism studied by NMR, proving a predominance of the *Z* isomer. It was possible to observe a isomers ratio, which LQOF-G2 presented 84.7% *Z* and 15.3% *E* [25].

Based on these reported results, it was synthetized two new guanidine compounds brominated. Hence, it was able to examine the effects of the additional bromine atoms into the structure on both, biological activity, and conformational ratio.

The new brominated guanidines were synthesized by reaction of a monobrominated guanidine with *N*-Bromosuccinimide (NBS) under IR irradiation. [26-31].

2. Results and Discussion

The aiming of this study was to investigate the increase of bromine atoms in guanidine compounds as potential antileishmanial agent. The biological activity of these new compounds is under study. On the other hand, conformational behavior was examined by NMR and XRD.

2.1. Guanidine bromination

Synthesis of LQOF-G2 and LQOF-G35 have been reported [20,22,24], for LQOF-G30 was used the same method. To preparation of the new brominated compound LQOF-G35-Br, it was used a catalyst free NBS reaction with IR activation at 150 Watts. NBS bromination of LQOF-G35 and LQOF-G2 yielded the same tri-brominated product.

2.2. Compounds characterization

Compounds were analyzed by Mass Spectrometry with electronic ionization allowed to observe molecular ions for the analyzed guanidines. The compounds were also studied by high resolution mass spectrometry with electrospray ionization in the positive ion mode (ESI(+)-MS) and was identified by the detection of their intact protonated molecule, which were selected and further fragmented via ESI(+)-MS/MS experiments. Figure S5 shows the HRESI(+)-MS and ESI(+)-MS/MS spectra of the compound LQOF-G35-Br (m/z 565.8898 [M+H]+). The ESI(+)-MS/MS experiments yielded fragment ions at m/z 487 and 365 that are in agreement with formation of the desired product.

NMR studies were performed at -10 °C (263 K) or -20 °C (253 K) for LQOF-G2, LQOF-G30, LQOF-G35 and LQOF-G35-Br. The NMR spectra can be found in the supplementary material and the most relevant data is highlighted in the Table 2.

Table 2. Chemical shifts (ppm) obtained by ^{1}H and ^{13}C NMR of guanidine compounds.

 doi:10.20944/preprints202312.1728.v2

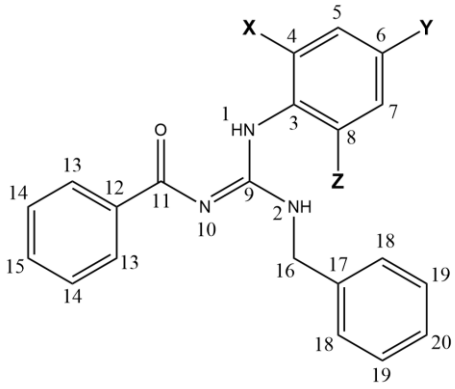

LQOF-G2	X = Z = H; **Y = Br**
LQOF-G35	**X = Br**; Y = Z = H
LQOF-G30	**X = Y = Br**; Z = H
LQOF-G35-Br	**X = Y = Z = Br**

HYDROGENS

	H1	H2	H1′	H2′	H5	H8	H13	H14	H16	H18
LQOF-G2	12.21	5.23	-	11.25	7.55	7.15	8.28	7.44	4.82	7.38
LQOF-G35	12.33	5.19	-	11.28	7.68	7.31	8.30	7.43	4.76	7.38
LQOF-G30	12.34	5.10	-	11.37	7.84	-	8.31	7.45	4.83	7.45
LQOF-G35-Br	12.26	5.31	8.61	9.64	7.71	-	8.28	7.48	4.82	7.56

CARBONS

	C3	C4	C6	C8	C9	C11	C12	C13	C14	C16	C17	C18
LQOF-G2	134.6	127.3	120.6	-	158.2	177.8	138.0	129.0	127.9	45.1	138.2	127.6
LQOF-G35	134.8	121.5	-	-	158.1	177.7	138.1	129.3	128.1	45.0	138.4	127.8
LQOF-G30	134.0	122.1	121.0	-	157.9	177.9	137.7	127.9	129.1	45.2	138.0	127.7
LQOF-G35-Br	119.3	115.4	143.3	115.4	144.4	166.8	132.6	127.0	127.6	45.0	138.0	129.1

2.3. Conformacional study

The ^{1}H NMR of LQOF-G35 revealed the signals of the hydrogens NH1 and NH2, with chemical shifts of 5.19 and 12.33 ppm, respectively. This was confirmed by HMBC ^{1}Hx^{15}N (Figure S20) and proved the Z isomer. LQOF-G30 showed the same signals at 5.10 and 12.34 ppm, corresponding to NH1 and NH2 respectively, but also showed a high intensity signal at 11.37 ppm (NH2') revealing the *E* isomer. In contrast, LQOF-G35-Br showed the signals at 8.61 and 9.64 ppm attributed to NH1' and NH2' with high intensity, that were associated to both *E* and *Z* isomers in solution. These measurements were conducted at -20 °C (253 K) and the results are shown in Table 3.

This difference is due to the stabilization of both conformations by the presence of a hydrogen bond between the hydrogen atom of the aniline or benzyl NH groups and the carbonyl oxygen atom, forming a pseudo six-membered cycle. In this way, the NH hydrogen atom involved in the intramolecular hydrogen bond becomes less shielded. Therefore, it is possible to confirm the conformational change from *Z* to *E* on the polybromination. This result was confirmed by XRD study (Figure 2).

Table 3. *E*/*Z* Isomer proportion (%) of guanidines compounds calculated by ^{1}H NMR at 253K.

Compound	*Isomer E %*	*Isomer Z %*
LQOF-G2	7.02	92.98
LQOF-G35	17.07	82.93
LQOF-G30	36.14	63.86
LQOF-G35-Br	53.54	46.46

It is possible to observe the increase of the isomer *E* population, in agreement with the raise of the bromine atoms in the aniline ring.

Compound LQOF-G35-Br showed a singlet that integrates two protons at 7.73 ppm. This signal is associated with hydrogens H5/H7, confirming the symmetry of the aniline tri-brominated ring. This observation was supported by HMBC ^{1}Hx^{13}C analysis that showed the correlations with four ^{13}C

 doi:10.20944/preprints202312.1728.v2

signals, where three of these can be associated with quaternary carbons (C4/C8 115.4 ppm, C3 119.3 ppm and C6 143.6 ppm), as well as with the carbon C5/C7, observed at 134.6 ppm.

Aliphatic hydrogens (H16) were identified by the signal at 4.7 ppm and was corroborated by the HSQC $^{1}Hx^{13}C$ study. Aromatic hydrogens were observed in the region of 7.0-8.5 ppm.

By ^{13}C NMR analysis it was possible to observe the aliphatic signal attributed to C16 for both compounds. In the regions of 115 and 166 ppm, were observed the signals of all remaining carbons. However, for LQOF-G35-Br an additional quaternary carbon signal was observed when compared with LQOF-G35.

In conjunction with these analyses, a NOESY study was performed. Figure 1 illustrates the main spatial correlations for investigated guanidines. It was possible to observe intense correlations between H2-H16 and H18-H16 for LQOF-G35, with emphasis on the H13-H16 and H8-H2 correlations, what indicate the *Z* conformation. For LQOF-G35-Br, intense correlations were observed between H1-H16, H18-H16 and H19-H16, therefore, indicating the *E* conformation.

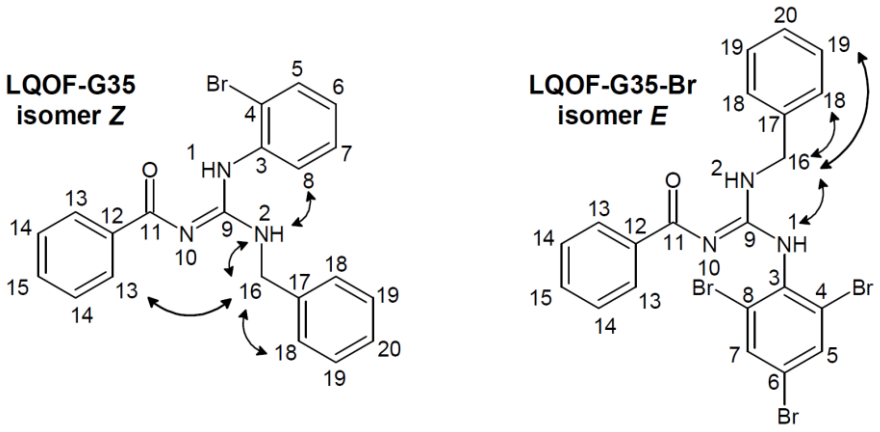

Figure 1. Conformational NOESY study of guanidines LQOF-G35 -*Z* isomer 98% - and LQOF-G35-Br -*E* isomer 56%- at 263 K.

Single crystals of both compounds were obtained and analyzed using the SCXRD technique. The compound LQOF-G35 crystallizes in the non-centrosymmetric trigonal space group $P3_2$ and contains three independent molecules in the asymmetric unit, as shown in Figure 2. The SCRXD study of LQOF-G35 show that the guanidine group present a resonant structure, with C–N bond distances ranging from 1.330 Å to 1.357 Å, formed by the contribution of the different resonance hybrids. As indicated by the NMR analyses, the LQOF-G35 has the *Z* conformation, with the amine group from the aniline stabilized by a six membered ring intramolecular hydrogen bond, N1H···O1. The presence of the hydrogen atoms bonded to the nitrogen atoms from the aniline and aminobenzyl groups was also indicated by the SCXRD analysis, with the evaluation of the electronic density maps.

 doi:10.20944/preprints202312.1728.v2

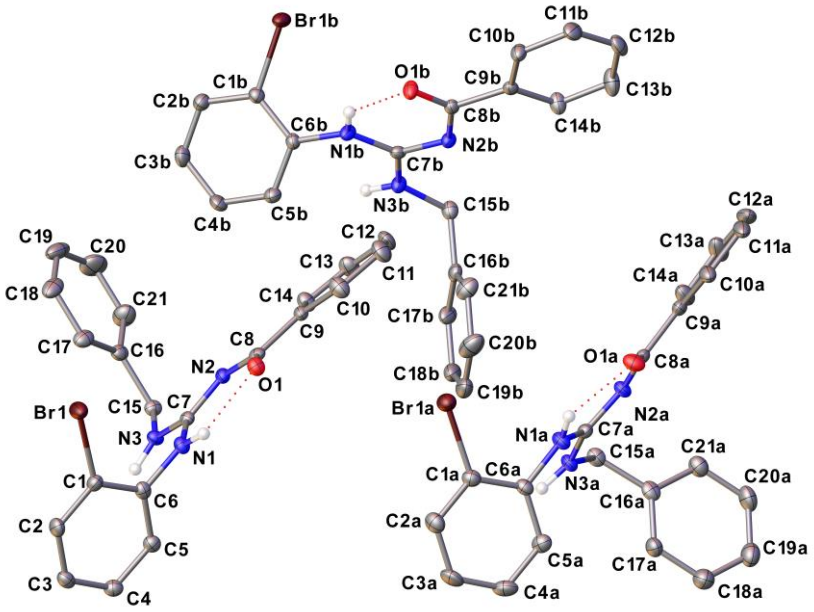

Figure 2. ORTEP type representation of the asymmetric unit of LQOF-G35, with thermal ellipsoids represented with 50% of probability. Hydrogen atoms bonded to the carbon atoms were omitted for clarity.

On the other hand, compound LQOF-G35-Br crystallized in the monoclinic space group $P2_{1/c}$, containing just one molecule per asymmetric unit (Figure 3). The analysis of the C-N bond lengths of the guanidine group, C7–N1 (1.290(3) Å), C7–N2 (1.409(3) Å) and C7–N3 (1.348(3) Å), indicate that the double bond is not in resonance in this case, just involving the atoms C7 and N1. An inversion in the position of the aniline and aminobenzyl groups was verified in the structure of LQOF-G35-Br, presenting an *E* conformation about the C7–N2, being now stabilized by another six membered ring intramolecular hydrogen bond, in this case involving N3H···O1. The electronic density maps analysis also confirmed the presence of the hydrogen atoms bonded to the nitrogen atoms N2 and N3.

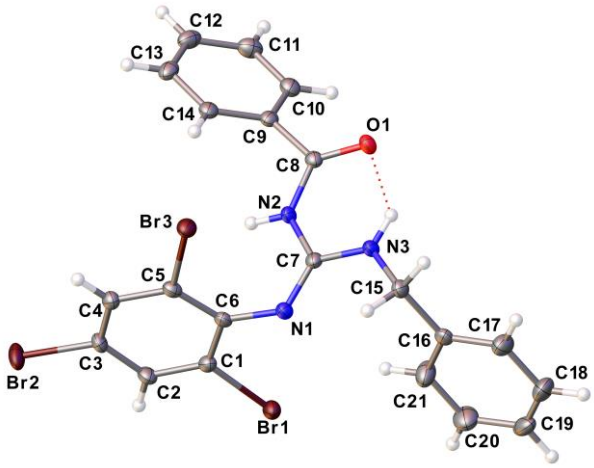

Figure 3. ORTEP type representation of the asymmetric unit of LQOF-G35-Br. Thermal ellipsoids are represented with 50% of probability.

To better understanding the conformational change, LQOF-G35 was subjected to 12 hours of infrared irradiation without NBS and subsequently analyzed by ^{1}H NMR. This experiment revealed that the initial *Z* conformation of LQOF-G35 was conserved. Therefore, the polybromination was responsible for the preferential *E* conformation observed in LQOF-G35-Br, more specifically the

 doi:10.20944/preprints202312.1728.v2

entrance of the second atom of bromo, which was confirmed because the compound with two bromine atoms in the aniline ring was synthesized and it showed only the *Z* conformation.

The *Z*/*E* conformational ratio is directly related to the position of the double bond N10=C9 (Figure 1). The entry of the second atom of bromo in the aniline moiety, promoted the rotation of the aniline ring and the breaking of the *pi* conjugation of the aniline nitrogen with the *pi*-aromatic cloud, because of the loss of p-p orbitals superposition (structures 3 and 4 in Scheme 1). Consequently, the free electrons-pair of the nitrogen can be conjugated toward the guanidine-central carbon, promoting the *pi* electrons migration until the opening of the carbonyl double bond and enolate formation. Therefore, the N10-C9 became a sigma bond allowing the rotation to reach the *E* conformation with the carbonyl double bound (keto form) regenerated and the N10=C9 double bond restored (structure 5 in Scheme 1). Finaly, a tautomer formed from the isomer *E* of compound LQOF-G35-Br crystallized and the corresponding monocrystal was measured by XRD (structure 6 in Scheme 1).

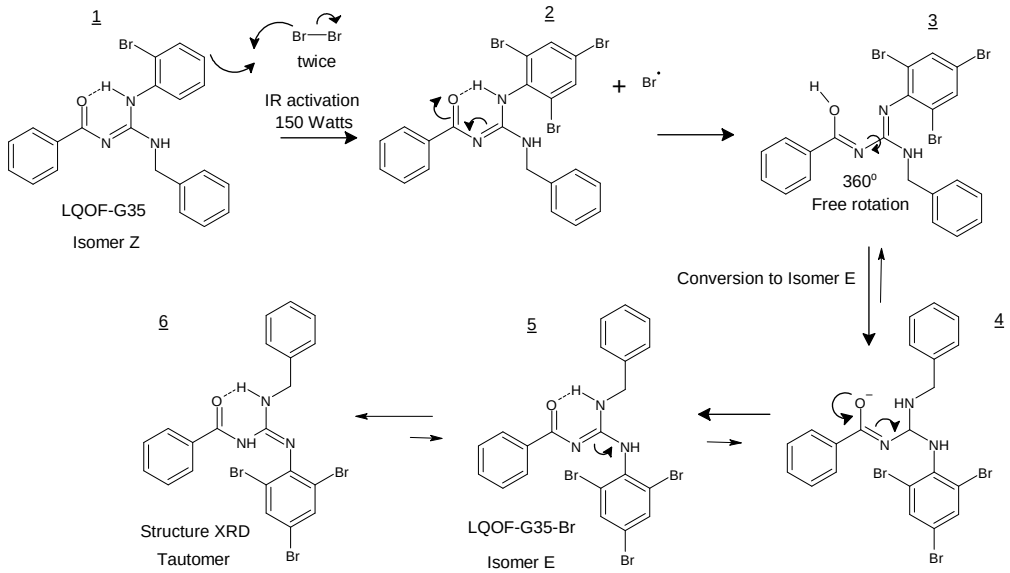

Scheme 1. Proposed mechanism pathway for conformational changes from LQOF-G35 to LQOF-G35-Br on bromination with NBS.

2.4. Structural data of compounds

(*Z*)-*N*-benzoyl-*N*-benzyl-*N*-(4-bromophenyl)guanidine (LQOF-G2). Yield of isolated product 69%. MM: 407.06 g.mol^{-1}. White solid. Melting point: 101.5-101.8°C. ^{1}H NMR 263K (500.16 MHz, $CDCl_3$) δ Z isomer = 12.21 (s, 1H), 8.28 (d, 2H), 7.54 (d, 1H), 7.50 (q, 2H), 7.44 (t, 3H), 7.40 – 7.34 (m, 4H), 7.33 (m, 1H), 7.16 (d, 1H), 5.23 (t, 1H), 4.82 (d, 2H). ^{13}C NMR (125.765 MHz, $CDCl_3$) δ = 177.8 (C=O), 158.2 (C=N), 138.2 (C), 137.9 (C), 134.6 (C), 133.2 (CH), 131.4 (CH), 129.0 (CH), 128.8 (CH), 128.7 (CH), 127.9 (CH), 127.6 (CH), 127.3 (CH), 127.2 (CH), 120.1 (C-Br), 45.1 (N-CH_2). δ E isomer = 11.25 (s, 1H). GC-MS/EI (m/z 406).

(*Z*)-*N*-benzoyl-*N*-benzyl-*N*-(2-bromophenyl)guanidine (LQOF-G35). Yield of isolated product 83%. MM: 407.06 g.mol^{-1}. White solid. Melting point: 103-104°C. ^{1}H NMR 263K (500.16 MHz, $CDCl_3$) δ Z isomer = 12.33 (s, 1H), 8.30 (d, 2H), 7.69 (d, 1H), 7.50 (q, 2H), 7.43 (t, 3H), 7.41 – 7.34 (m, 4H), 7.31 (m, 1H), 7.16 (t, 1H), 5.19 (t, 1H), 4.84 (d, 2H). ^{13}C NMR (125.765 MHz, $CDCl_3$) δ = 177.7 (C=O), 158.1 (C=N), 138.2 (C), 137.8 (C), 134.6 (C), 134.0 (CH), 131.4 (CH), 129.1 (CH), 128.8 (CH), 128.7 (CH), 127.9 (CH), 127.6 (CH), 127.5 (CH), 127.4 (CH), 121.2 (C-Br), 45.0 (N-CH_2). δ E isomer = 11.28 (s, 1H). GC-MS/EI (m/z 406). ESI(+)-MS *m*/*z* found 408.0705, *m*/*z* calculated for $[C_{21}H_{18}BrN_3O + H]^+$: 408.0706; ESI(+)-MS/MS: M+H – $C_6H_5CONH_2]^+$ *m*/*z* 287.0175, $[M+H - C_{15}H_{12}N_2O]^+$ *m*/*z* 171.9757, $[M+H - C_{13}H_{12}BrN_2]^+$ *m*/*z* 122.0603.

(*Z*)-*N*-benzoyl-*N*-benzyl-*N*-(2,4-dibromophenyl)guanidine (LQOF-G30). Yield of isolated product 71%. MM: 487.19 g.mol^{-1}. White solid. Melting point: 130.6 – 131.4°C. ^{1}H NMR 263K (500.16 MHz, $CDCl_3$) δ Z isomer = 12.34 (s, 1H), 8.31 (d, 2H), 7.84 (s, 2H), 7.71 – 7.24 (m, 19H), 5.10 (t, 1H),

 doi:10.20944/preprints202312.1728.v2

4.83 (d, 2H), 4.67 (t, 2H). ^{13}C NMR (125.765 MHz, $CDCl_3$) δ = 177.9 (C=O), 157.9 (C=N), 138.0 (C), 137.8 (C), 136.4 (C), 134.0 (CH), 131.7 (CH), 129.1 (CH), 128.8 (CH), 128.3 (CH), 127.9 (CH), 127.7 (CH), 127.1 (CH), 122.1 (CH), 121.0 (C-Br), 45.2 (N-CH_2). δ E isomer = 11.37 (s, 1H). LC-UV/MS: 99.82%; ESI(+)-MS: m/z 485.9812, m/z calculated [C21H16Br2N3O+H]+: 487.9790; ESI(+)-MS/MS [M+H – C6H5C(O)NH2]+ m/z 366.9258.

(*E*)-*N*-benzoyl-*N*-benzyl-*N*-(2,4,6-*tri*-bromophenyl)guanidine (LQOF-G35-Br). Yield of isolated product 60%. MM: 566.09 g.mol-1. White solid. Melting point: 148-149°C. ^{1}H NMR 263K (500.16 MHz, $CDCl_3$) δ *E* isomer 9.64 (s, 1H), 8.63 (s, 1H), 8.29 (d, 2H), 7.78 – 7.64 (m, 4H), 7.61 – 7.53 (m, 4H), 7.53 – 7.22 (m, 20H) 7.16 (t, 1H), 5.31 (t, 1H), 4.83 (d, 2H);; δ *Z* isomer 12.26 (s, 1H), 5.31 (s, 1H). ^{13}C NMR (125.765 MHz, $CDCl_3$) δ = 166.8 (C=O), 144.4 (C=N), 143.3 (C-Br), 138.0 (C), 134.5 (CH), 133.2 (CH), 132.6 (C), 129.1 (CH), 128.6 (CH), 127.9 (CH), 127.6 (CH), 127.0 (CH), 119.3 (C), 115.4 (2C-Br), 45.0 (N-CH2). δ Z isomer = 12.26 (s, 1H), 5.31 (s, 1H). GC-MS/EI (m/z 565): 77, 91, 105, 122, 285, 406, 486. HRESI-MS m/z 565.8898 [M+H]+ (calcd for C21H16Br3N3O1, 566.091, Δ= -0.2012 ppm). Ionic fragment observed in ESI(+)-MS/MS: [M+H–$C_{14}H_{11}BrN_2O$]+ m/z 486.5555.

3. Materials and Methods

3.1. Guanidine bromination using NBS and IR irradiation

N-Bromosuccinimide (NBS) and Infrared activation were used (Scheme 2). The reaction was performed using a molar relationship guanidine:NBS of 1 mol of guanidine to 1.4 mol of NBS. After 12 h the reaction mixture was cooled to 10 °C and washed with water, then the organic layer (dichloromethane) was separated and dried on magnesium sulfate. The dried organic solution was filtered off, the solvent was evaporated, and the product was recrystallized from a mixture of petroleum ether and diethyl ether (9:1 v/v). Then, the resulting suspension was filtered off and the solid was dried by reduced pressure and suspended in ethanol with ultrasound and recrystallized one more time. Bromination was also carried out from LQOF-G2 under the same experimental conditions. Both starting guanidines, LQOF-G35 and LQOF-G2 yielded the same product, LQOF-G35-Br.

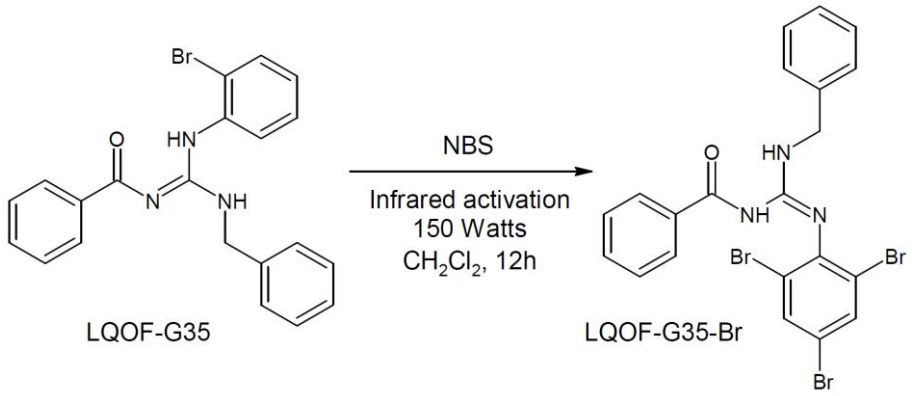

Scheme 2. Bromination of the compound LQOF-G35 with formation of the polybrominated compound LQOF-G35-Br as confirmed by XRD.

3.2. Melting point

Melting point was obtained using a WRS-2 Micro Processor Melting-point apparatus. The samples were placed in a capillary tube, and pre-heating and final ramp temperatures were selected for 60 °C and 250 °C, respectively. The heating rate used was 2.0 °C/min.

3.3. Electronic ionization mass spectrometry

The mass spectra of the guanidines were acquired by direct introduction (DI) in the Mass Spectrometry, with a Shimadzu QP-2010 Plus equipment with Electron Ionization (EI). The parameters used for the analysis were: Interface temperature: 240°C; Ionization chamber: 300 °C;

 doi:10.20944/preprints202312.1728.v2

Time to solvent cut; 0.5 min; Initial time: 0.7 min; Final time: 25 min; DI temperature program: Initial temperature: 50 °C, with heating from 20 °C/min to 350 °C and standby time 10 min. The analysis was performed using acetonitrile and dichloromethane as a solvent. The energy used for ionization was 70 eV.

3.4. NMR

^{1}H, ^{13}C and other 2D NMR spectra were recorded on a Bruker Avance III-HD – 500 MHz. The resonance frequency for ^{1}H NMR was 500.16 MHz and for ^{13}C NMR 125.765 MHz. Chemical shifts for ^{1}H NMR and ^{13}C NMR were referenced to TMS, analysis was performed in $CDCl_3$ and all chemical shifts were reported in ppm. Data are presented as following: chemical shift, multiplicity (s = singlet, d = doublet, dd = doublet of doublet, t = triplet, qua = quadruplet, qu = quintuplet, m = multiplet, br s = broad singlet), integration, and coupling constants (in Hertz).

3.5. HRESIMS

The UPLC-ESI-QTOF-MS/MS analysis was performed on a Waters modular UHPLC consisting of a QSM Acquity® HClass quaternary pump, an Acquity® Sample Manager – FTM autosampler, and an Acquity® PDAeλ diode array detector, hyphenated to a Waters Xevo® G2-XS mass spectrometer, equipped with an electrospray ionization source (ESI), a quadrupole analyzer, and a collision cell configured in sequence with a time-of-flight (TOF) analyzer. The chromatographic separation was performed in gradient mode using a solution of formic acid at 0.1% v/v as mobile phase in ultrapure water as component A and acetonitrile acidified with formic acid at a concentration of 0.1% v/v as component B. Chromatographic runs were performed at a flow rate of 0.5 mL.min-1, starting with 5% of component B in the mobile phase composition. The variation of the elution force was programmed so that in 5 min the %B increased until reaching the value of 100%. The analysis was performed on a Waters Acquity® UPLC HSS T3 reversed phase column (C18) containing 1.8 µm particles with 2.1 mm internal diameter and 100 mm length. The injection volume applied to the column was 0.2 µL. Full scan and MS/MS mass spectra were acquired in positive mode in the range of m/z 100 to 1500. Electrospray capillary and transfer cone voltages were maintained at (+) 2.5 kV and 20 V respectively. The ESI source and desolvation gas temperatures were set to 120.0 and 350.0 °C respectively. The acquisition of MS/MS spectra was performed in Fast DDA mode (data dependent acquisition), in which only ions with intensity above 100 were fragmented. Ion fragmentation was performed by applying a voltage ramp so that for m/z 100 the energy ranged from 10 to 40 eV and for m/z 1500, from 40 to 70 eV.

3.6. Single crystal X-ray diffraction (SCXRD)

Single crystals of LQOF-G35 and LQOF-G35-Br were obtained and analyzed at 100 K on a Rigaku XtaLAB Synergy-S Dualflex diffractometer equipped with an HyPix 6000HE detector, using a Cu Kα radiation (1.54184 Å). Data collection, cell refinement, data reduction and absorption correction were performed using the CrysAlisPro software [32]. Intrinsic phasing method from the SHELXT-2018/2 program [33] was used to solve the structures, while the refinement of the non-hydrogen atoms was performed with non-linear the least-squares minimization on F^2 using the SHELXL-2019/2 program [34] and considering anisotropic displacement parameters. Hydrogen atoms were calculated at idealized positions using the riding model. The calculated positions of the hydrogen atoms bonded to the nitrogen atoms from the guanidine group were confirmed by the analyses of the electron density maps. Olex2 [35] was used for the solution and refinement of the structures, and to generate the graphical illustrations. Tables containing the information about the data collection, refinement and structural parameters are available in the Supplementary Materials.

The CIF file of LQOF-G35 and LQOF-G35-Br were deposited in the Cambridge Structural Data Base with CCDC number 2320314 and 23200315, respectively. Copies of the data can be obtained, free of charge, via www.ccdc.cam.ac.uk or https://www.ccdc.cam.ac.uk/structures/?access=referee.

4. Conclusions

 doi:10.20944/preprints202312.1728.v2

Bromated compounds LQOF-G2, LQOF-G35, LQOF-G30 and LQOF-G35-Br were synthesized in satisfactory to good yields All the compounds have been unambiguously characterized.

Low-temperature NMR and single crystal XRD have confirmed that all the bromine atoms are in the aniline ring. A conformational change from *Z* to *E* is also observed, being promoted, and raised by the growth in the number of bromine atoms in the aniline ring.

The XRD analysis revealed that the compound with three bromine atoms on the aniline moiety, LQOF-G35-Br, crystallized as a tautomer directly formed from the *E* isomer.

Supplementary Materials: The following supporting information can be downloaded at: www.mdpi.com/xxx/s1, Figure S1: EI-MS (70 eV) spectrum of compound LQOF-G2; Figure S2: EI-MS (70 eV) spectrum of compound LQOF-G35; Figure S3: EI-MS (70 eV) spectrum of compound LQOF-G30; Figure S4: EI-MS (70 eV) spectrum of compound LQOF-G35-Br; Figure S5: HRESI-MS Spectrum of LQOF-G35-Br; Figure: S6: HPLC-UV analysis of LQOF-G30; Figure: S7: HPLC-UV analysis of LQOF-G35; Figure: S8: HRESI-(+) MS analysis of LQOF-G30; Figure: S9: HRESI-(+) MS analysis of LQOF-G35; Figure: S10: HRESI-(+) MS/MS analysis of LQOF-G35; Figure S11: ^{1}H NMR spectrum for LQOF-G2 at 263K in $CDCl_3$; Figure S12: ^{13}C DEPTQ-135 NMR spectrum for LQOF-G2 at 263K in $CDCl_3$; Figure S13: HSQC ^{1}Hx^{13}C NMR spectrum for LQOF-G2 at 263K in $CDCl_3$; Figure S14: HMBC ^{1}Hx^{13}C NMR spectrum for LQOF-G2 at 263K in $CDCl_3$; Figure S15: NOESY ^{1}Hx^{1}H NMR spectrum for LQOF-G2 at 263K in $CDCl_3$; Figure S16: ^{1}H NMR spectrum for LQOF-G35 at 263K in $CDCl_3$; Figure S17: ^{13}C DEPTQ-135 NMR spectrum for LQOF-G35 at 263K in $CDCl_3$; Figure S18: HSQC ^{1}Hx^{13}C NMR spectrum for LQOF-G35 at 263K in $CDCl_3$; Figure S19: HMBC ^{1}Hx^{13}C NMR spectrum for LQOF-G35 at 263K in $CDCl_3$; Figure S20: HMBC ^{1}Hx^{15}N NMR spectrum for LQOF-G35 at 263K in $CDCl_3$; Figure S21: NOESY ^{1}Hx^{1}H NMR spectrum for LQOF-G35 at 263K in $CDCl_3$; Figure S22: ^{1}H NMR spectrum for LQOF-G30 at 263K in $CDCl_3$; Figure S23: ^{13}C DEPTQ-135 NMR spectrum for LQOF-G30 at 263K in $CDCl_3$; Figure S24: HSQC ^{1}Hx^{13}C NMR spectrum for LQOF-G30 at 263K in $CDCl_3$; Figure S25: HMBC ^{1}Hx^{13}C NMR spectrum for LQOF-G30 at 263K in $CDCl_3$; Figure S26: NOESY ^{1}Hx^{1}H NMR spectrum for LQOF-G30 at 263K in $CDCl_3$; Figure S27: ^{1}H NMR spectrum for LQOF-G35-Br at 263K in $CDCl_3$; Figure S28: ^{13}C DEPTQ-135 NMR spectrum for LQOF-G35-Br at 263K in $CDCl_3$; Figure S29: HSQC ^{1}Hx^{13}C NMR spectrum for LQOF-G35-Br at 263K in $CDCl_3$; Figure S30: HMBC ^{1}Hx^{13}C NMR spectrum for LQOF-G35-Br at 263K in $CDCl_3$; Figure S31: NOESY ^{1}Hx^{1}H NMR spectrum for LQOF-G35-Br at 263K in $CDCl_3$; Figure S32: ^{1}H NMR spectrum for LQOF-G2 at 253K in $CDCl_3$ to %*E*/*Z*; Figure S33: ^{1}H NMR spectrum for LQOF-G35 at 253K in $CDCl_3$ to %*E*/*Z*; Figure S34: ^{1}H NMR spectrum for LQOF-G30 at 253K in $CDCl_3$ to %*E*/*Z*; Figure S35: ^{1}H NMR spectrum for LQOF-G35-Br at 253K in $CDCl_3$ to %*E*/*Z*; Table S1: Crystal data and refinement parameters of LQOF-G35 and LQOF-G35-Br; Table S2: Selected bond lengths and angles for LQOF-G35; Table S3: Selected bond lengths and angles for LQOF-G35-Br.

Author Contributions: E.H.Z.—organic synthesis and, NMR conformational study; L.R.d.A.— organic synthesis and NMR conformational study; E.H.Z. and L. R. d. A. have the same contributions; P.H.O.S. — X-ray measurements and process for conformational study; T.R.d.S.N. — organic synthesis; J.A.E — X-ray measurements, process for conformational study and supervision; E.R.P.G.—general supervision. All authors have read and agreed to the revised version of the manuscript.

Funding: This research received no external funding.

Data Availability Statement: No applicable.

Acknowledgments: Eduardo Henrique Zampieri and Luana Ribeiro dos Anjos thanks to CAPES for postgraduation fellowships. Eduardo R. P. Gonzalez thanks to FAPESP for financial support (funding 2021/0595-8) and to UNESP–MCTI-IEAMAR and FAPESP (2018/00581-7 and 2021/2595-8) for 500 MHz Bruker NMR apparatus. Eduardo R. Perez Gonzalez is thankful to Agreement FINEP 01.23.0034.00 (0419/22) – "Study and identification of active compounds against cutaneous and visceral leishmaniasis: from discovery to preclinical study", Process FUNDUNESP - CCP nº 3348/2022. Pedro H. O. Santiago thanks to FAPESP (2021/10066-5). Javier Ellena is grateful to FAPESP (2017/15850-0) and CNPq (312505/2021-3).

Conflicts of Interest: The authors declare no conflict of interest.

References

1. World Health Organization, Leishmaniasis. Available online: https://www.who.int/news-room/fact-sheets/detail/leishmaniasis (accessed on 02 December 2023).

 doi:10.20944/preprints202312.1728.v2

2. Abadías-Granado, I.; Diago,4.; Cerro, P. A.; Palma-Ruiz,A. M.; Gilaberte, Y. Cutaneous and Mucocutaneous Leishmaniasis. *Actas Dermo-Sifiliográficas (English Edition)* **2021**, *112*, 601-618.
3. Cecílio, P.; Cordeiro-da-Silva, A.; Oliveira, F. Sand flies: Basic information on the vectors of leishmaniasis and their interactions with Leishmania parasites. *Commun Biol*. **2022**, *5*, 305.
4. Ikeogu, N.M.; Akaluka, G.N.; Edechi, C.A.; Salako, E.S.; Onyilagha, C.; Barazandeh, A.F.; Uzonna, J.E. Leishmania Immunity: Advancing Immunotherapy and Vaccine Development. *Microorganisms* **2020**, *8*, 1201.
5. Pradhan, S.; Schwartz, R. A.; Patil, A.; Grabbe, S.; Goldust, M. Treatment options for leishmaniasis. *CED* **2022**, *47*, 516–521.
6. Basmaciyan, L.; Casanova M. Cell death in Leishmania. *Parasite* **2019**, *26*, 71.
7. Spasov, A.; Ozerov, A.; Kosolapov, V.; Gurova, N.; Kucheryavenko, A.; Naumenko, L.; Babkov, D.; Sirotenko, V.; Taran, A.; Borisov, A.; et al. Guanidine Derivatives of Quinazoline-2,4(1H,3H)-Dione as NHE-1 Inhibitors and Anti-Inflammatory Agents. *Life* **2022**, *12*, 1647.
8. Morrill, C.; Friesen, W. J.; Babu, S.; Baiazitov, R. Y; Du, W. et al. Guanidino quinazolines and pyrimidines promote readthrough of premature termination codons in cells with native nonsense mutations. *Bioorganic & Medicinal Chemistry Letters* **2022**, *76*, 128989.
9. Yoshida, Y.; Endo, T. Synthesis of multifunctional 4-hydroxymethyl 2-oxazolidinones from glycidyl carbamate derivatives catalyzed by bicyclic guanidine. *Tetrahedron Letters* **2021**, *72*, 153086.
10. Shakaroun, R. M.; Jéhan, P.; Alaaeddine, A.; Carpentier, J.; Guillaume, S. M. Organocatalyzed ring-opening polymerization (ROP) of functional β-lactones: new insights into the ROP mechanism and poly(hydroxyalkanoate)s (PHAs) macromolecular structure. *Polym. Chem.* **2020**, *11*, 2640-2652.
11. Mesías-Salazar, Á.; Martínez, J.; Rojas, R. S.; Carrillo-Hermosilla, F.; Ramos, A.; Fernández-Galánb, R.; Antiñolo, A. Aromatic guanidines as highly active binary catalytic systems for the fixation of CO2 into cyclic carbonates under mild conditions. *Catal. Sci. Technol.* **2019**, *9*, 3879-3886.
12. Korolkova, Y.; Makarieva, T.; Tabakmakher, K.; Shubina, L.; Kudryashova, E.; Andreev, Y.; Mosharova, I.; Lee, H.-S.; Lee, Y.-J.; Kozlov, S. Marine Cyclic Guanidine Alkaloids Monanchomycalin B and Urupocidin A Act as Inhibitors of TRPV1, TRPV2 and TRPV3, but not TRPA1 Receptors. *Mar. Drugs* **2017**, *15*, 87.
13. Staszewski, M.; Iwan, M.; Werner, T.; Bajda, M.; Godyń, J.; Latacz, G.; Korga-Plewko, A.; Kubik, J.; Szałaj, N.; Stark, H.; et al. Guanidines: Synthesis of Novel Histamine H3R Antagonists with Additional Breast Anticancer Activity and Cholinesterases Inhibitory Effect. *Pharmaceuticals* **2023**, *16*, 675.
14. Siddiqui, M. A.; Nagargoje, A. A.; Shaikh, M. H.; Siddiqui, R. A.; Pund, A. A.; Khedkar, V. M. et al. Design, Synthesis and Bioevaluation of Highly Functionalized 1,2,3-Triazole-Guanidine Conjugates as Anti-Inflammatory and Antioxidant Agents. *Polycyclic Aromatic Compounds* **2023**, *43*, 5567-5581.
15. Zubair, S.; Badshah, A.; Patujo, J.; Khan, M.; Raheel, A.; Asghar, F.; Imtiaz, S. New ferrocene integrated amphiphilic guanidines: Synthesis, spectroscopic elucidation, DFT calculation and in vitro α-amylase and α-glucosidase inhibition combined with molecular docking approach. *Heliyon* **2023**, *9*, e14919.
16. Cao, Y. ; Gu, J. ; Wang, S. et al. Guanidine-functionalized cotton fabrics for achieving permanent antibacterial activity without compromising their physicochemical properties and cytocompatibility. *Cellulose* **2020**, *27*, 6027–6036.
17. Zhang, X.; Han, D.; Pei, P.; Hao, J.; Lu, Y. et al. In vitro Antibacterial Activity of Isopropoxy Benzene Guanidine Against Multidrug-Resistant Enterococci. *Infection and Drug Resistance* **2019**, *12*, 3943-3953.
18. Baugh, S.D.P. Guanidine-Containing Antifungal Agents against Human-Relevant Fungal Pathogens (2004–2022)—A Review. *J. Fungi* **2022**, *8*, 1085.
19. Gomes, A. R.; Varela, C. L.; Pires, A. S.; Tavares-da-Silva, E. J.; Roleira, F. M. F. Synthetic and natural guanidine derivatives as antitumor and antimicrobial agents: A review. *Bioorganic Chemistry* **2023**, *138*, 106600.
20. Espírito Santo, R. D.; Velásquez, Á. M. A.; Passianoto, L. V. G.; Sepulveda, A. A. L.; Clementino, L. C. et al. N, N`, N``-trisubstituted guanidines: Synthesis, characterization and evaluation of their leishmanicidal activity. *European Journal of Medicinal Chemistry* **2019**, *171*, 116e128.
21. Costa, N. C. S.; Anjos, L. R.; Souza, J. V. M.; Brasil, M. C. O. A.; Moreira, V. P. et al. Development of New Leishmanicidal Compounds via Bioconjugation of Antimicrobial Peptides and Antileishmanial Guanidines. *ACS Omega* **2023**, 8, 34008–34016.
22. Moreira, V.P.; da Silva Mela, M.F.; Anjos, L.R.; Saraiva, L.F.; Arenas Velásquez, A.M.; Kalaba, P.; Fabisiková, A.; Clementino, L.d.C.; Aufy, M.; Studenik, C.; et al. Novel Selective and Low-Toxic Inhibitor of LmCPB2.8ΔCTE (CPB) One Important Cysteine Protease for Leishmania Virulence. *Biomolecules* **2022**, *12*, 1903.
23. Almeida, F.S.; Moreira, V.P.; Silva, E.d.S.; Cardoso, L.L.; de Sousa Palmeira, P.H.; Cavalcante-Silva, L.H.A.; Araújo, D.A.M.d.; Amaral, I.P.G.d.; González, E.R.P.; Keesen, T.S.L. Leishmanicidal Activity of Guanidine Derivatives against Leishmania infantum. *Trop. Med. Infect. Dis.* **2023**, *8*, 141.
24. Anjos, L. R.; de Souza, V. M. R.; Machado, Y. A. A.; Partite, V. M.; Aufy, M.; Dias-Lopes, G.; studenik, C.; Alves, C. R.; Lubec, G.; González, E. R. P.; Rodrigues, K. A. F. Evidence of guanidines potential against

 doi:10.20944/preprints202312.1728.v2

Leishmania (Viannia) braziliensis: Exploring in vitro effectiveness, toxicities and of innate immunity response effects. *Biomolecules* **2023**, *14*, 26.

25. Espírito Santo, R. D.; Simas, R. C.; Magalhães, A. et al. Experimental NMR and MS study of benzoylguanidines. Investigation of E/Z isomerism. *Journal of Physical Organic Chemistry* **2013**, 26, 4, 315-321.
26. Isac-García, J.; Dobado, J. A.; Calvo-Flores, F. G.; Martínez-García, H. *Experimental Organic Chemistry: Laboratory Manual*. 1st ed.; Academic Press: USA, 2015; pp. 371-408.
27. Ram, V. J.; Sethi, A.; Nath, M.; Pratap, R. *The Chemistry of Heterocycles*. 1st ed.; Elsevier: Cambridge, USA, 2019; pp. 149–478.
28. Barnes, R. A. N-Bromosuccinimide as a Dehydrogenating Agent1. *Journal of the American Chemical Society* **1948**, *70*, 145–147.
29. Sivakamasundari, S.; Ganesan, R. Kinetics and mechanism of the bromination of aromatic compounds byN-bromosuccinimide in solution. *International Journal of Chemical Kinetics* **1980**, *12*, 837–850.
30. Appa, R.M. ; Naidu, B.R. ; Lakshmidevi, J. et al. Added catalyst-free, versatile and environment beneficial bromination of (hetero)aromatics using NBS in WEPA. *SN Appl. Sci.* **2019**, *1*, 1281.
31. Lee, S.; Ra, C. S. Benzylic Brominations with N-Bromosuccinimide in 1,2-Dichlorobenzene: Effective Preparation of (2-Bromomethyl-phenyl)-Methoxyiminoacetic Acid Methyl Ester. *Clean Technol.* **2016**, *22*, 269-273.
32. Oxford Diffraction /Agilent Technologies UK Ltd CrysAlisPRO.
33. Sheldrick, G.M. SHELXT – Integrated space-group and crystalstructure determination. *Acta Cryst*. **2015**, *A71*, 3–8.
34. Sheldrick, G.M. Crystal structure refinement with SHELXL. *Acta Cryst.* **2015**, *C71*, 3–8.
35. Dolomanov, O. V.; Bourhis, L. J.; Gildea, R. J.; Howard, J. A. K.; Puschmann, H. Olex2: A complete structure solution, refinement and analysis program. *J. Appl. Cryst.* **2009**, *42*, 339-341.